IOPscience iopscience.iop.org

Home Search Collections Journals About Contact us My IOPscience

Electron Emission Properties of GaAsN/GaAs Quantum Well Containing N-Related Localized States: The Influence of Illuminance

This content has been downloaded from IOPscience. Please scroll down to see the full text.

2012 Jpn. J. Appl. Phys. 51 02BJ12

(http://iopscience.iop.org/1347-4065/51/2S/02BJ12)

View the table of contents for this issue, or go to the journal homepage for more

Download details:

IP Address: 140.113.38.11
This content was downloaded on 28/04/2014 at 21:49

Please note that terms and conditions apply.

Japanese Journal of Applied Physics **51** (2012) 02BJ12 **REGULAR PAPER**
DOI: 10.1143/JJAP.51.02BJ12

Electron Emission Properties of GaAsN/GaAs Quantum Well Containing N-Related Localized States: The Influence of Illuminance

Meng-Chien Hsieh*, Jia-Feng Wang, Yu-Shou Wang, Cheng-Hong Yang, Chen-Hao Chiang, and Jenn-Fang Chen

Department of Electrophysics, National Chiao Tung University, Hsinchu, Taiwan 30050, Republic of China

Received September 26, 2011; accepted October 25, 2011; published online February 20, 2012

This study elucidates the electron emission properties of GaAsN/GaAs quantum well containing N-related localized states under illumination. The N-related localized states in a GaAsN quantum well (QW) are identified as both optical and electrical electron trap states. The mechanisms for the responses of current–voltage (I–V) measurement under illumination and photocapacitance are investigated. N-related localized states in GaAsN QW can extend response range and response sensitivity on photocapacitance, and produce an additional current path for photo-generated electron–hole pairs. Furthermore, exactly how illumination influences the electron emission rate of GaAsN QW electron state is examined. The electron emission rate of GaAsN QW electron state can be modulated by different incident photon energy, which is due to the modulation of depletion width of the bottom GaAs. © 2012 The Japan Society of Applied Physics

1. Introduction

III–V alloys containing nitrogen (commonly referred to as dilute nitrides), such as $GaAs_{1-x}N_x$ and $In_yGa_{1-y}As_{1-x}N_x$, have received considerable attention experimentally and theoretically in the recent decade. They are characterized by a large decrease of the band gap upon incorporation of a small amount of nitrogen.[1–7] III–V alloys are thus promising materials for applications such as vertical cavity surface-emitting lasers that are operated in the coveted 1.3–1.5 μm range[8–12] and high efficiency multijunction solar cells.[13–17] However, nitrogen atoms result in a carrier localization effect at low temperatures, often making photoluminescence (PL) weaker than in a N-free system.[18] As is well known, the optical quality of dilute nitrides can be improved using rapid thermal annealing (RTA).[19–23] However, even for annealed materials, low-temperature PL spectra obtained at low excitation conditions are dominated by the recombination of localized carriers (excitons) that are trapped at local potential minima (N-related localized states).[24,25] Nevertheless, to our knowledge, the exact nature of N-related localized states in GaAsN/GaAs quantum well (QW) under illumination is still controversial. Hence, understanding the electron emission properties of GaAsN/GaAs QW containing N-related localized states under illumination is particularly worthwhile, from both physics and device design perspectives.

This study investigates the influence of illumination on the electron emission properties of GaAsN/GaAs QW containing N-related localized states by current–voltage (I–V) measurement under illumination, Photocapacitance measurement, and admittance spectroscopy. The N-related localized states are identified by optical and electrical measurements. The responses of I–V measurement under illumination and photocapacitance are also investigated. Furthermore, exactly how illumination influences the electron emission rate of GaAsN QW electron state is examined.

2. Experiments

GaAsN/GaAs SQW samples were grown on n^+-GaAs(001) substrates by molecular beam epitaxy (MBE). An EPI-Unibulb radio frequency (rf) plasma source was used to provide nitrogen species from a pure N_2 gas. The gallium was supplied from conventional Knudsen effusion cells; As in the form of As_2 was supplied from a cracker source. The growth was started with a 0.3 μm Si-doped GaAs layer of 4×10^{16} cm^{-3} grown at 580 °C, followed by a 8-nm-thick GaAsN layer, grown at 480 °C. To avoid the introduction of any unwanted shallow impurity states, the GaAsN layer was undoped. After the growth of the GaAsN layer, the growth temperature was increased to 580 °C for the growth of a 0.3 μm Si-doped GaAs top layer of 4×10^{16} cm^{-3}. The N composition was estimated by the PL peak energy to be about 2.7%. Schottky contact was established by evaporating Al on the samples with a dot diameter of 800 μm. Admittance spectroscopy was performed using a HP 4194A impedance analyzer.

3. Results and Discussion

Figure 1(a) shows the power-dependent PL spectra (at 30 K) of the 8 nm as-grown sample. In this figure, two broad emission peaks appear at 1.16 and 1.03 eV. Comparing these results with the annealing result [Fig. 1(b)] reveals that the broad emission peak appearing at the high-energy side (1.16 eV) is GaAsN QW emission peak. A previous study identified the broad emission peak at 1.03 eV as associated with emission between the GaAsN QW electron states and a deep defect level at about 190 meV above the GaAs valence band.[26] Figure 1(b) shows the power-dependent PL spectra (at 30 K) of the 8 nm sample after RTA at 800 °C for 3 min. According to Figs. 1(a) and 1(b), RTA splits the broad as-grown GaAsN QW emission into two peaks, a low energy peak (1.17 eV) and a high energy peak (1.20 eV). Additionally, thermal annealing increases the PL intensity of the GaAsN QW emission and reduces the PL linewidth of the GaAsN QW emission. As is well known, post-growth thermal annealing significantly improves the quality of the alloy. Moreover, annealing of the bulk GaAsN layers increases PL intensity and reduces PL linewidth. Thus, the broad emission peak appearing at the high-energy side (1.16 eV) in as-grown sample is identified as GaAsN QW emission peak. Also, the high energy peak (1.20 eV) in RTA samples is also identified as GaAsN QW emission peak. Furthermore, the low energy peak (1.17 eV) exhibits a limited-filling feature relative to GaAsN QW emission peak. According to the limited-filling feature and the relative emission peak position, this low energy emission is the typical emission from N-related localized states.[24,25,27,28]

*E-mail address: markvipmail@yahoo.com.tw

 © 2012 The Japan Society of Applied Physics

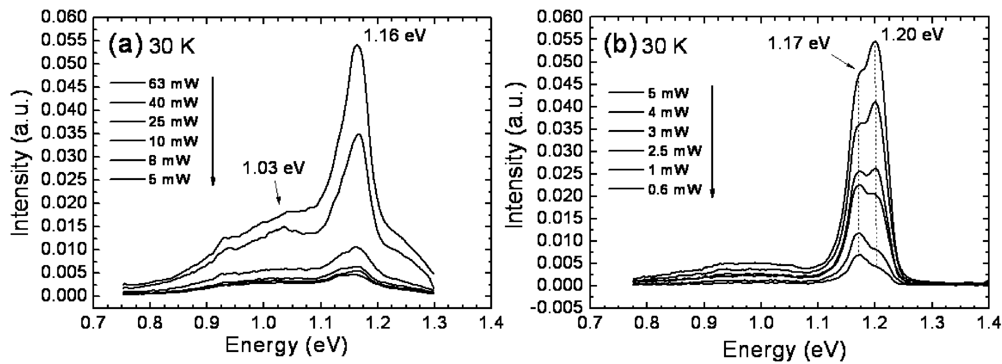

Fig. 1. (a) 30 K power-dependent PL spectra of the 8 nm as-grown sample. (b) 30 K power-dependent PL spectra of the 8 nm sample after RTA at 800 °C for 3 min.

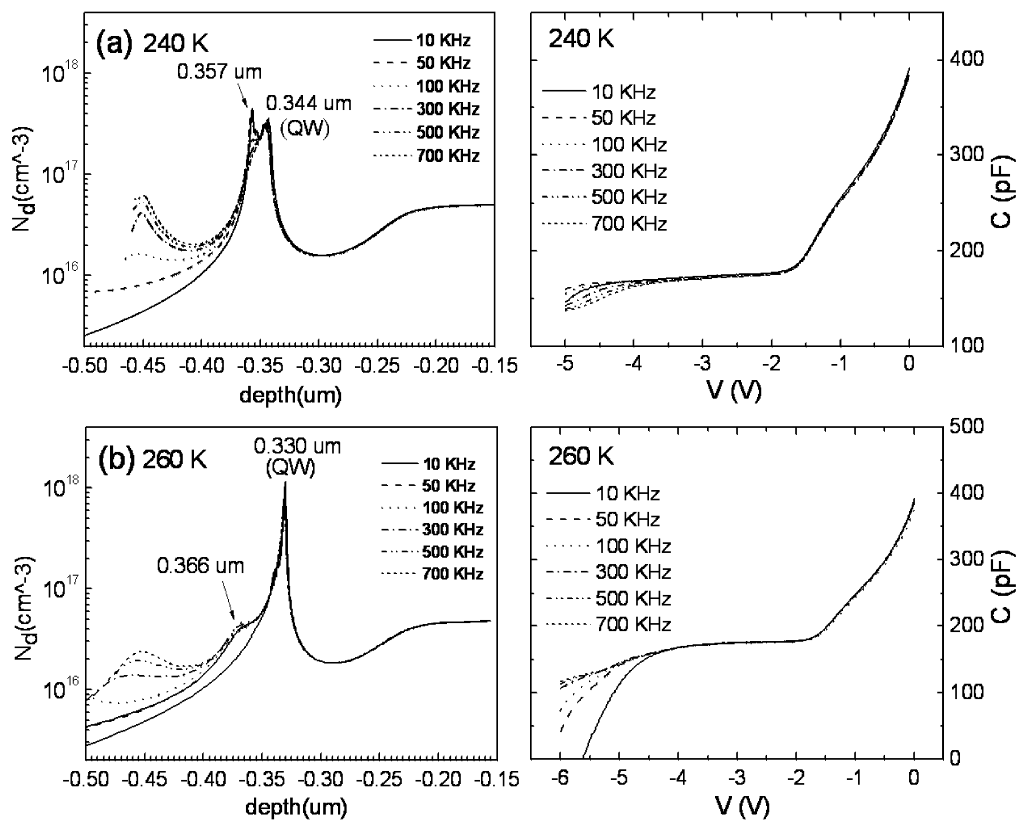

Fig. 2. (a) 240 K *C*–*V* depth profiles and the corresponding *C*–*V* spectra (as shown on the right side) of the 8 nm as-grown sample. (b) 260 K *C*–*V* depth profiles and the corresponding *C*–*V* spectra (as shown on the right side) of the 8 nm RTA 800 °C sample.

Figure 2 shows the capacitance–voltage (*C*–*V*) depth profiles [at (a) 240 K and (b) 260 K] and the corresponding *C*–*V* spectra (as shown on the right side) of the 8 nm (a) as-grown and (b) RTA 800 °C samples. In Fig. 2(a), two concentration peaks appear at 0.344 μm (*C*–*V* step at ∼−1.5 V) and 0.357 μm (*C*–*V* step at ∼−3.5 V) simultaneously in the as-grown sample. The depth of the shallow peak (0.344 μm) is close to the growth position of the GaAsN QW (∼0.3 μm). Notably, increasing the annealing temperature raises the intensity of this peak and reduces its linewidth. These results imply that the thermal annealing improves the carrier-confinement ability of the GaAsN QW electron states, and also conform to the influence of thermal annealing on the GaAsN QW PL emission. Furthermore, the electron emission time of this peak is restored to the short time constant after thermal annealing (not shown here), which exhibits a typical electron emission property of high-quality QW. The shallow peak is thus confirmed as the GaAsN QW electron states signal. Based on the Schottky depletion theory,[29] the concentration peak at the left side (deep side) of the QW peak indicates that the electron trap states of this peak is below the QW electron states. Additionally, the distance between the two concentration peaks corresponds to the energy separation between the two electron states. Moreover, increasing the annealing temperature reduces the deep peak intensity [from 4.3×10^{17} cm^{-3} (as-grown) to 4.6×10^{16} cm^{-3} (RTA 800 °C)] and increases the distance between the GaAsN QW peak and the deep

© 2012 The Japan Society of Applied Physics

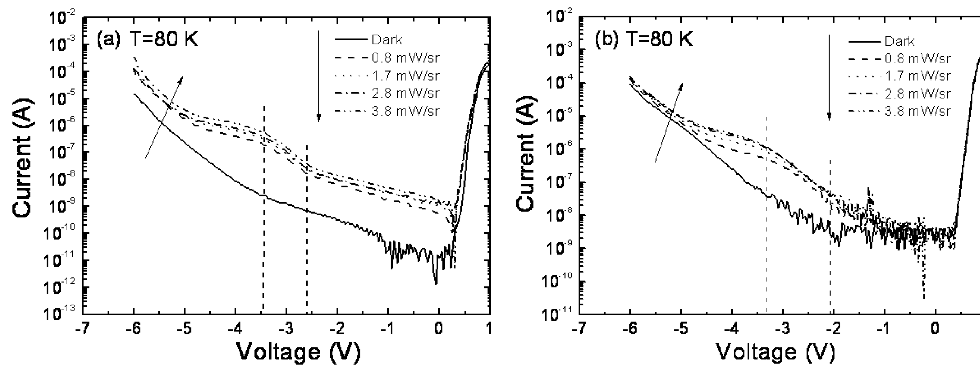

Fig. 3. I–V spectra (at 80 K) of the 8 nm (a) as-grown and (b) RTA 800 °C samples under different radiant intensity of $\lambda = 940$ nm (1.319 eV) LED illumination.

peak. These results indicate that thermal annealing reduces the electron trap states of the deep peak. Therefore, the electron trap states exhibit the same behaviors as the N-related localized states, suggesting that the deep peak originates from the electron emission of the N-related localized states. Thus, more than just optical electron trap states, the N-related localized states are also electrical electron trap states.

So far, we have investigated the optical and electrical properties of GaAsN/GaAs QW containing N-related localized states. We now turn to examine the influence of illuminance on electron emission properties of GaAsN QW containing N-related localized states. Figure 3 shows the I–V spectra (at 80 K) of the 8 nm (a) as-grown and (b) RTA 800 °C samples under different radiant intensity of $\lambda =$ 940 nm (1.319 eV) light-emitting diode (LED) illumination. In Fig. 3(a), the reverse-bias current is increased at all reverse-bias region after LED illumination, and is attributed to the defect states in the GaAs region. The details of these defect states in the GaAs region will not be discussed here. In addition to the current rise from the defect states in the GaAs region, two stages of current rise are observed after LED illumination. The bias (at around -2.6 V) of the first current rise corresponds to the bias range of GaAsN QW electron states in above measurement, and the bias (at around -3.5 V) of the second current rise corresponds to the bias range of N-related localized states in above measurement. The similar result is also observed in RTA 800 °C sample, as shown in Fig. 3(b). In RTA 800 °C sample, the current rise from the defect states in the GaAs region is not observed. This result indicates that thermal annealing diminishs the defect states in the GaAs region. Similarly, the biases of the two stages of current rise are also corresponds to the bias ranges of GaAsN QW electron states and N-related localized states. The observation of I–V measurement under illumination suggests that both GaAsN QW electron states and N-related localized states can provide current path for photo-generated electron–hole pairs.

Photocapacitance measurement is utilized in further investigation of the electron emission properties of GaAsN QW containing N-related localized states under illumination. Figure 4 shows the photocapacitance spectra (at 80 K) and the corresponding PL spectra (as shown on the below) of the 8 nm (a) as-grown and (b) RTA 800 °C samples. These photocapacitance measurements were held at (a) -1 V $f = 150$ kHz for as-grown sample and (b) -2.5 V $f =$ 500 kHz for RTA 800 °C sample. As mentioned earlier, the capacitance signals under these biases represent the electron emission behavior of electron on GaAsN QW electron states. In Fig. 4(a), as the energy of the incident photon is increased, photocapacitance started falling. This fall in photocapacitance is usual in GaAs layer and is attributed to emission from the hole traps A and B located at energies 0.4 and 0.7 eV, respectively, above the valence band.[30] Further increasing the energy of the incident photon, a obvious rise of photocapacitance start at 1.08 eV which indicates the electron emission from electron states. The end of the photocapacitance rise at 1.08 eV is around 1.32 eV. According to the PL measurement results, this energy range of photocapacitance rise corresponds to the broad emission peak of GaAsN QW which is composed of the emission from GaAsN QW and N-related localized states. Thus, the photocapacitance rise between 1.08 and 1.32 eV is attributed to the electron emission from GaAsN QW electron states and N-related localized states. The other changes of photocapacitance after 1.32 eV are probably originated from the other electron traps and hole traps in GaAs layer which will not be discussed here. After thermal annealing, as shown in Fig. 4(b), the photocapacitance features an initial photocapacitance rise at around 0.7 eV which is due to emission from the electron trap in GaAsN layer observed before.[31] Thus, as the energy of the incident photon is increased, the photocapacitance spectrum is dominated by the electron trap in GaAsN layer and the usual hole traps in GaAs layer, resulting in a bump of photocapacitance at initial. Further increasing the energy of the incident photon, two stages of photocapacitance rise are observed at 1.16 and 1.22 eV. According to the PL measurement results, the observed energys at 1.16 and 1.22 eV are correspond to the emission energys of GaAsN QW and N-related localized states. Hence, the two stages of photocapacitance rise are attributed to the electron emission from GaAsN QW electron states and N-related localized states. The other changes of photocapacitance after 1.32 eV are same as as-grown sample which will not be discussed here. Moreover, the photocapacitance rises originated from GaAsN QW electron states and N-related localized states can be separately distinguished, and the photocapacitance rise caused by GaAsN QW electron states is larger than the photocapacitance rise caused by N-related localized states. This results also

© 2012 The Japan Society of Applied Physics

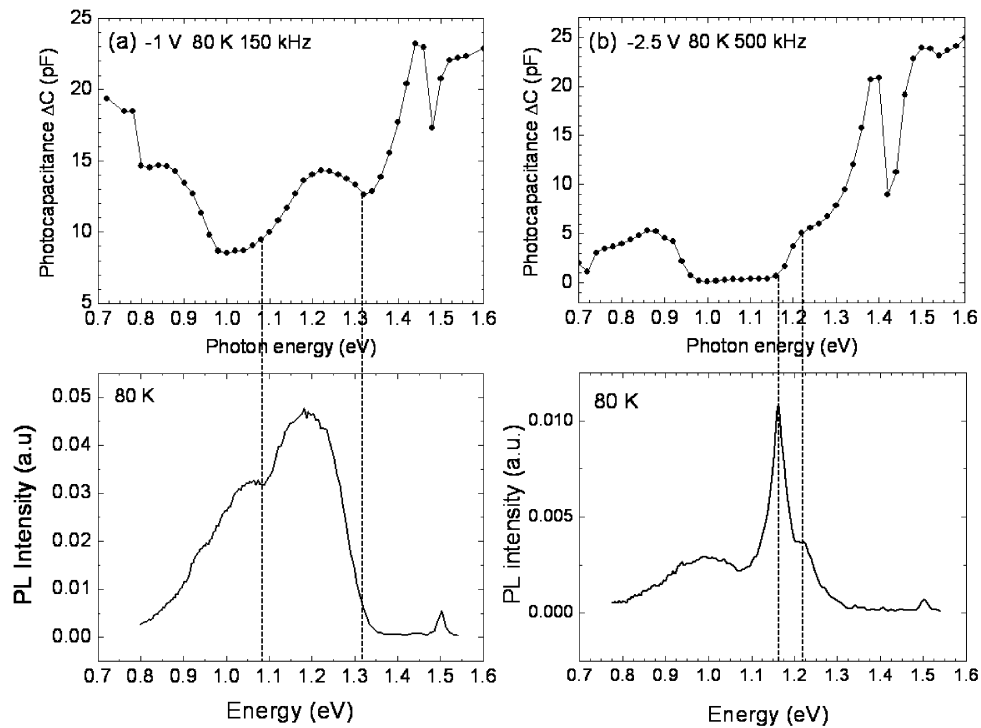

Fig. 4. Photocapacitance spectra (at 80 K) and the corresponding PL spectra (as shown on the below) of the 8 nm (a) as-grown and (b) RTA 800 °C samples.

conform to the optical and electrical properties that we have investigated above. In above results, the emissions of GaAsN QW electron states and N-related localized states can be separated after thermal annealing; the electron states of GaAsN QW are more than N-related localized states, leading to the dominance of GaAsN QW emission on the PL spectra at high excitation. Therefore, the existence of N-related localized states in GaAsN QW can provide more electron states to modify the characteristics of photocurrent and photocapacitance. In GaAsN QW, N-related localized states can extend response range and response sensitivity on photocapacitance, and produce an additional current path for photo-generated electron–hole pairs. Furthermore, the properties of N-related localized states can be modulated by controlling N-composition fluctuation, different growth conditions, and post-growth thermal annealing. Thus, the application of N-related localized states is a feasibility method for device design of opto-electronic devices.

The mechanism of the photocapacitance rise from GaAsN QW electron states is examined in detail below. Figure 5 shows the schematic band diagrams for illustrating the photocapacitance rise from GaAsN QW electron states. Before illumination, Fermi level intersects with the GaAsN QW electron states for a carrier modulation, as shown in Fig. 5(a). Based on the Schottky depletion theory,[29] the capacitance is originated from the depletion width W_{d1} which is related to the carrier concentration of GaAsN QW electron states and GaAs layer. At the beginning of illumination, the incident photons generate the electron–hole pairs on GaAsN QW states, as shown in Fig. 5(b). Since the carrier concentrations of photon-generation electrons and holes are equal at the beginning of illumination, the net charges in the depletion region are equivalent to the sample before illumination. Thus, the depletion width W_{d1} is not changed at the beginning of illumination. Because the emission rate of electron on GaAsN QW states is faster than the emission rate of hole on GaAsN QW states, photon-generation electrons on GaAsN QW states are less than photon-generation holes on GaAsN QW states when illumination achieving the steady-state. Therefore, this non-equilibrium carrier distribution of photon-generation electron–hole pairs can be regarded as a escape of part of photon-generation electrons, as shown in Fig. 5(c). The photon-generation electrons escaping into bottom GaAs will cause the change of net charges in the bottom GaAs, resulting in a decrease of depletion region of bottom GaAs. Thus, the depletion width after illumination decreases to W_{d2} ($W_{d2} < W_{d1}$), leading to a rise of capacitance after illumination. Incidentally, from the Schottky depletion theory,[29] we also can obtain the voltage drop of GaAs bottom layer as follows:

$$V_1 = \frac{qN_d(W_{d1} - W_{QW})^2}{2\varepsilon_s},$$

$$V_2 = \frac{qN_d(W_{d2} - W_{QW})^2}{2\varepsilon_s},$$

where N_d is the background concentration in the GaAs bottom layer, W_{QW} is the designed QW position from the surface, and ε_s is the permittivity of the semiconductor. Therefore, the decrease of depletion region of bottom GaAs also decreases the voltage drop of GaAs bottom layer. In the Schottky depletion theory, the voltage drop of GaAs bottom layer is correspond to the position of Fermi level. Hence, the change of voltage drop is correspond to the shift of Fermi level position ($\Delta E_F = V_1 - V_2$), and this result will be utilized later. In addition, it is worth to mention that Kondow *et al.* have reported the decreased permittivity due to N incorporation,[32] and thus the permittivity of GaAsN layer is

© 2012 The Japan Society of Applied Physics

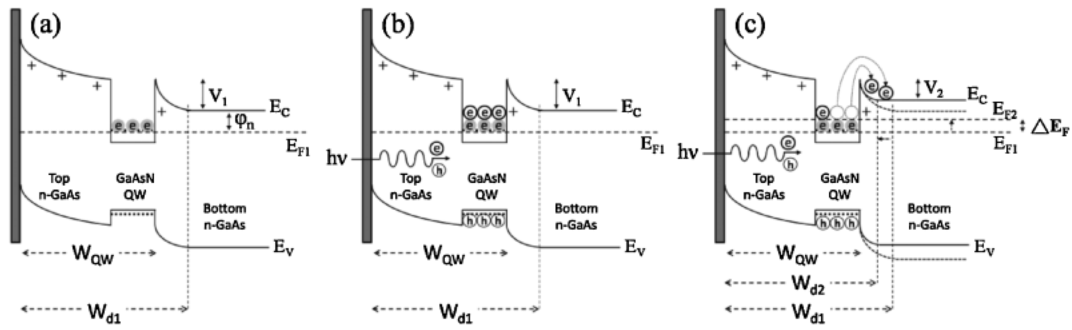

Fig. 5. The schematic band diagrams of GaAsN/GaAs QW structure under applied bias (a) before illumination, (b) at the beginning of illumination, and (c) when illumination achieving the steady-state.

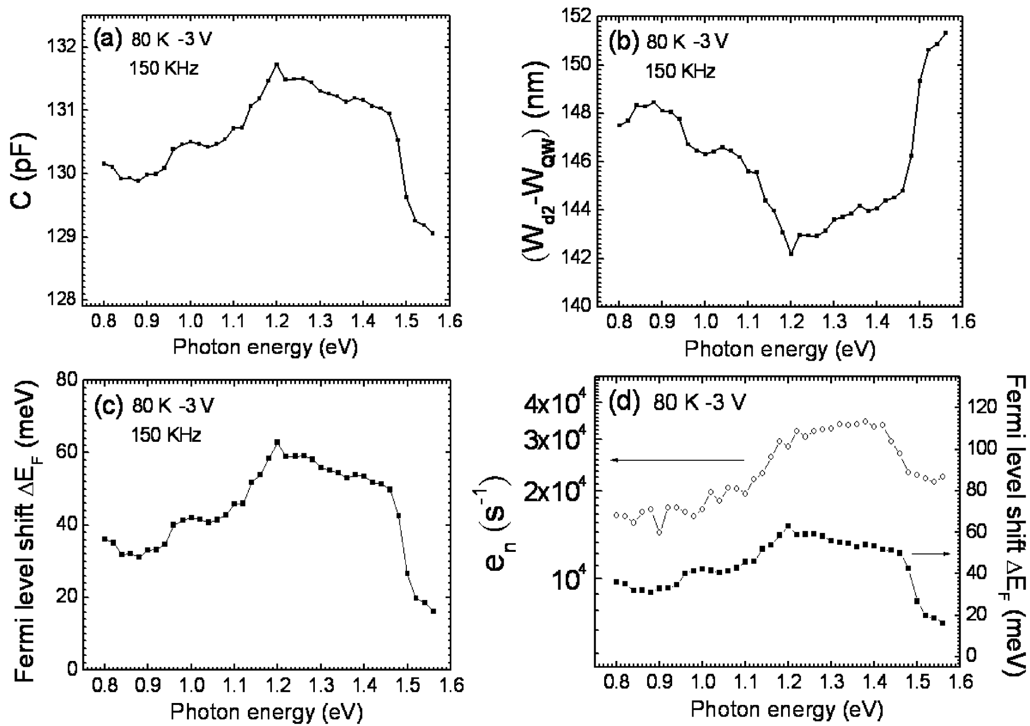

Fig. 6. (a) Photon energy–capacitance spectrum (at 80 K) of the 8 nm as-grown sample, held at -3 V 150 kHz. (b) Spectrum for depletion width of the bottom GaAs ($W_{d2} - W_{QW}$) under different incident photon energy. (c) Spectrum for the Fermi level shift (ΔE_F) under different incident photon energy. (d) Plots of the e_n vs photon energy (open circle) and ΔE_F vs photon energy (solid circle) obtained from the C–F measurement and (c).

not the same as that of GaAs layer. However, as comparing with the top GaAs layer (300 nm), the proportion of GaAsN layer (8 nm) is relatively small, and our analysis is focused on the variation in depletion region of bottom GaAs. Therefore, for simplicity, the influence of the variation in the permittivity of GaAsN layer was ignored in our analysis.

We now turn to examine the influence of illuminance on electron emission rate of GaAsN QW electron state. Figure 6(a) shows the photon energy–capacitance spectrum (at 80 K) of the 8 nm as-grown sample, held at -3 V 150 kHz. The capacitance signal under this bias is correspond to a carrier modulation of GaAsN QW electron states. As above-mention, based on the Schottky depletion theory,[29] the depletion width of the bottom GaAs ($W_{d2} - W_{QW}$) under different incident photon energy can be extracted from Fig. 6(a), as shown in Fig. 6(b). In addition, according to this theory, the shift of Fermi level position (ΔE_F) under different incident photon energy also can be extracted from Fig. 6(b), as shown in Fig. 6(c). Thus, the photon-generation electrons escaping into bottom GaAs will cause the change of net charges in the bottom GaAs, resulting in the shift of Fermi level position. Next, we utilize the model of thermally activated process[33] to analyze the correlation between electron emission rate of GaAsN QW and illuminance. According to this model, the electron emission rate (e_n) is exponentially proportional to the confined energy (ΔE), which is given by

$$e_n = \gamma T^2 \sigma_\infty \exp\left(-\frac{\Delta E}{KT}\right),$$

where σ_∞ is the capture cross section for $T = \infty$, and γ is a temperature-independent constant. Based on the Schottky depletion theory, the confined energy ΔE can be obtained as follows:

© 2012 The Japan Society of Applied Physics

$$\Delta E = V + \varphi_n,$$

where V is the voltage drop of GaAs bottom layer, and φ_n is the Fermi potential. Thus, the electron emission rate (e_n) is just exponentially proportional to the Fermi level shift (ΔE_F), which is consistent with the form

$$e_n = \gamma T^2 \sigma_\infty \exp\left[\frac{-(V_1 + \varphi_n - \Delta E_F)}{KT}\right] \sim \exp(\Delta E_F).$$

Therefore, the shift of Fermi level position by different incident photon energy will modulate the electron emission rate of GaAsN QW electron state. Admittance spectroscopy (C–F) measurement was performed to obtain electron emission rate (e_n) of GaAsN QW electron state under different incident photon energy, and the obtained electron emission rates (e_n) are shown in Fig. 6(d) (open circle). Figure 6(d) plots the e_n vs photon energy (open circle) and ΔE_F vs photon energy (solid circle) spectra. The Fermi level shift in Fig. 6(d) are obtained from the Fig. 6(c), which is correspond to the modulation of depletion width of the bottom GaAs under different incident photon energy. According to Fig. 6(d), the variation of electron emission rate under different incident photon energy exhibits a similar behavior to the Fermi level shift under different incident photon energy, and follows the relation form: $e_n \sim \exp(\Delta E_F)$. Thus, the electron emission rate of GaAsN QW electron state can be modulated by different incident photon energy, which is due to the modulation of Fermi level position in the GaAsN QW. These results indicate that GaAsN QW containing N-related localized states is suitable for application of high sensitive photodetector. The variation of electron emission time constant can reach twice under different incident photon energy. Therefore, the variation of electron emission time constant can be utilized to distinguish the incident photon energy. Incidentally, as mentioned earlier, the PL linewidth of the GaAsN QW emission is broad in our as-grown sample. The broad PL linewidth of the GaAsN QW emission indicates that the GaAsN QW electron states have a broad distribution. Hence, this finding indicates that the GaAsN QW electron states are widely distributed above the GaAsN CB, explaining why we can observe the variation of electron emission rate during the shift of Fermi level position.

4. Conclusions

This study elucidates the electron emission properties of GaAsN/GaAs QW containing N-related localized states under illumination. Initially, the N-related localized states are identified by optical and electrical measurements. The N-related localized states in a GaAsN quantum well are identified as both optical and electrical electron trap states. Next, the mechanisms for the responses of I–V measurement under illumination and photocapacitance are probed. Thus, N-related localized states in GaAsN QW can extend response range and response sensitivity on photocapacitance, and produce an additional current path for photo-generated electron–hole pairs. The application of N-related localized states is a feasibility method for device design of opto-electronic devices. Furthermore, we investigate the influence of illuminance on electron emission rate of GaAsN QW electron state. The electron emission rate of GaAsN QW electron state can be modulated by different incident photon energy, which is due to the modulation of depletion width of the bottom GaAs. This result also indicate that GaAsN QW containing N-related localized states is suitable for application of high sensitive photodetector. The variation of electron emission time constant can be utilized to distinguish the incident photon energy.

Acknowledgements

The authors would like to thank the National Science Council of the Republic of China, Taiwan, for financially supporting this research under Contract No. NSC-97-2112-M-009-014-MY3, as well as the MOE ATU program for its support.

1) S. Sakai, Y. Ueta, and Y. Teauchi: Jpn. J. Appl. Phys. **32** (1993) 4413.
2) M. Kondow, S. Nakatsuka, T. Kitatani, Y. Yazawa, and M. Okai: Electron. Lett. **32** (1996) 2244.
3) S. H. Wei and A. Zunger: Phys. Rev. Lett. **76** (1996) 664.
4) W. G. Bi and C. W. Tu: Appl. Phys. Lett. **70** (1997) 1608.
5) S. Sato, Y. Osawa, and T. Saitoh: Jpn. J. Appl. Phys. **36** (1997) 2671.
6) L. Bellaiche and A. Zunger: Phys. Rev. B **57** (1998) 4425.
7) T. Kitatani, M. Kondow, T. Kikawa, Y. Yazawa, M. Okai, and K. Uomi: Jpn. J. Appl. Phys. **38** (1999) 5003.
8) M. C. Larson, M. Kondow, T. Kitatani, K. Nakahara, K. Tamura, H. Inoue, and K. Uomi: IEEE Photonics Technol. Lett. **10** (1998) 188.
9) J. S. Harris, Jr.: Semicond. Sci. Technol. **17** (2002) 880.
10) M. Kondow, T. Kitatani, K. Nakahara, and T. Tanaka: Jpn. J. Appl. Phys. **38** (1999) L1355.
11) S. Sato and S. Satoh: J. Cryst. Growth **192** (1998) 381.
12) N. Tansu and L. J. Mawst: IEEE Photonics Technol. Lett. **14** (2002) 444.
13) M. Bosi and C. Pelosi: Prog. Photovoltaics **15** (2007) 51.
14) J. Z. Li, J. Y. Lin, H. X. Jiang, J. F. Geisz, and S. R. Kurtz: Appl. Phys. Lett. **75** (1999) 1899.
15) A. J. Ptak, S. W. Johnston, S. Kurtz, D. J. Friedman, and W. K. Metzger: J. Cryst. Growth **251** (2003) 392.
16) S. R. Kurtz, J. F. Geisz, B. M. Keyes, W. K. Metzger, D. J. Friedman, J. M. Olson, R. R. King, and N. H. Karam: Appl. Phys. Lett. **82** (2003) 2634.
17) T. H. Wu, Y. K. Su, Y. C. Lin, and Y. J. Wang: Jpn. J. Appl. Phys. **45** (2006) L647.
18) M. Henini: *Dilute Nitride Semiconductors* (Elsevier, Amsterdam, 2005) Chap. 4.
19) E. V. K. Rao, A. Ougazzaden, Y. Le Bellego, and M. Juhel: Appl. Phys. Lett. **72** (1998) 1409.
20) S. Francoeur, G. Sivaraman, Y. Qiu, S. Nikishin, and H. Temkin: Appl. Phys. Lett. **72** (1998) 1857.
21) H. P. Xin, K. L. Kavanagh, Z. Q. Zhu, and C. W. Tu: Appl. Phys. Lett. **74** (1999) 2337.
22) L. H. Li, Z. Pan, W. Zhang, Y. W. Lin, Z. Q. Zhou, and R. H. Wu: J. Appl. Phys. **87** (2000) 245.
23) D. Kwon, R. J. Kaplar, S. A. Ringel, A. A. Allerman, S. R. Kurtz, and E. D. Jones: Appl. Phys. Lett. **74** (1999) 2830.
24) I. A. Buyanova, W. M. Chen, G. Pozina, J. P. Bergman, B. Monemar, H. P. Xin, and C. W. Tu: Appl. Phys. Lett. **75** (1999) 501.
25) R. Kudrawiec, G. Sek, J. Misiewicz, L. H. Li, and J. C. Harmand: Eur. Phys. J.: Appl. Phys. **27** (2004) 313.
26) J. F. Chen, C. T. Ke, P. C. Hsieh, C. H. Chiang, W. I. Lee, and S. C. Lee: J. Appl. Phys. **101** (2007) 123515.
27) I. A. Buyanova, W. M. Chen, B. Monemar, H. P. Xin, and C. W. Tu: Mater. Sci. Eng. B **75** (2000) 166.
28) X. D. Luo, Z. Y. Xu, W. K. Ge, Z. Pan, L. H. Li, and Y. W. Liu: Appl. Phys. Lett. **79** (2001) 958.
29) D. K. Schroder: *Semiconductor Material and Device Characterization* (Wiley, New York, 2006).
30) K. Mallik and S. Dhar: Phys. Status Solidi B **184** (1994) 393.
31) S. Dhar, N. Halder, J. Kumar, and B. M. Arora: Appl. Phys. Lett. **85** (2004) 964.
32) M. Kondow, M. Uchiyama, M. Morifuji, S. Wu, H. Momose, S. Fukushima, A. Fukuyama, and T. Ikari: Appl. Phys. Express **2** (2009) 041003.
33) D. V. Lang: J. Appl. Phys. **45** (1974) 3023.

© 2012 The Japan Society of Applied Physics